

The effects of hard-spectra solar proton events on the middle atmosphere

A. Seppälä,^{1,2} M. A. Clilverd,¹ C. J. Rodger,³ P. T. Verronen,² and E. Turunen⁴

Received 20 June 2008; revised 5 September 2008; accepted 16 September 2008; published 15 November 2008.

[1] The stratospheric and mesospheric impacts of the solar proton events of January 2005 are studied here using ion and neutral chemistry modeling and subionospheric radio wave propagation observations and modeling. This period includes three SPEs, among them an extraordinary solar proton storm on 20 January, during which the >100 MeV proton fluxes were unusually high, making this event the hardest in solar cycle 23. The radio wave results show a significant impact to the lower ionosphere/middle atmosphere from the hard spectrum event of 20 January with a sudden radio wave amplitude decrease of about 10 dB. Results from the Sodankylä Ion and Neutral Chemistry model predict large impacts on the mesospheric NO_x (400–500%) and ozone (–30 to –40% NH, –15% SH) in both the northern (winter) and the southern (summer) polar regions. The direct stratospheric effects, however, are only about 10–20% enhancement in NO_x, which result in –1% change in O₃. Imposing a much larger extreme SPE lasting 24 hours rather than just 1 hour produced only about 5% ozone depletion in the stratosphere. Only a massive hard-spectra SPE with high-energy fluxes over ten times larger than observed here (>30 MeV fluence of 1.0×10^9 protons/cm²), as, e.g., the Carrington event of 1859 (>30 MeV fluence of 1.9×10^{10} protons/cm²), could presumably produce significant in situ impacts on stratospheric ozone.

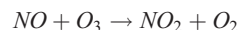
Citation: Seppälä, A., M. A. Clilverd, C. J. Rodger, P. T. Verronen, and E. Turunen (2008), The effects of hard-spectra solar proton events on the middle atmosphere, *J. Geophys. Res.*, 113, A11311, doi:10.1029/2008JA013517.

1. Introduction

[2] Solar proton events (SPE) originate from solar coronal mass ejections (CME), during which large amounts of protons and heavier ions are emitted from the Sun [Reames, 1999], sometimes toward the Earth. Solar protons that enter the Earth's magnetosphere are guided by the Earth's magnetic field to the polar cap areas where they can precipitate into the atmosphere [Patterson *et al.*, 2001; Rodger *et al.*, 2006]. Since the protons can have very high energies, up to hundreds of MeVs, they are able to deposit their energy in the mesosphere and stratosphere. Therefore solar proton events provide a direct connection between the Sun and the Earth's middle atmosphere. Though the occurrence of solar proton events can be sparse and irregular, they are extreme examples of solar forcing on the middle atmosphere.

[3] In the atmosphere, through ionization of the ambient air, the precipitating particles produce odd hydrogen (HO_x, H + OH + HO₂) and odd nitrogen (NO_x, N + NO + NO₂)

[Crutzen *et al.*, 1975; Solomon *et al.*, 1981; Rusch *et al.*, 1981] both of which have an important role in the ozone balance of the middle atmosphere. The HO_x and NO_x constituents take part in odd oxygen (O_x, O + O₃) destruction through catalytic reactions [e.g., Lary, 1997; Brasseur and Solomon, 2005, pp. 401–416], such as



[4] The produced HO_x has a relatively short lifetime of only a few days, but the chemical loss of NO_x takes place through photodissociation and is therefore dependent on solar irradiation levels. Thus, in conditions of low-level solar illumination, such as polar winter, NO_x may remain at an elevated level for long periods after a solar proton event. Significant depletion of middle atmospheric ozone during and after large solar proton events has been predicted by atmospheric modeling [e.g., Rusch *et al.*, 1981; Solomon *et al.*, 1983; Reid *et al.*, 1991; Jackman *et al.*, 1995, 2000; Verronen *et al.*, 2005] and has been observed by satellite measurements [e.g., Thomas *et al.*, 1983; McPeters and Jackman, 1985; Jackman *et al.*, 2001; Seppälä *et al.*, 2004, 2006, 2007; Randall *et al.*, 2005; López-Puertas *et al.*, 2005; Verronen *et al.*, 2006].

[5] In this paper we examine the effects of the January 2005 solar storms on the mesosphere and stratosphere and the D region of the ionosphere. The January events were

¹Physical Sciences Division, British Antarctic Survey, Natural Environment Research Council, Cambridge, UK.

²Finnish Meteorological Institute, Helsinki, Finland.

³Department of Physics, University of Otago, Dunedin, New Zealand.

⁴Sodankylä Geophysical Observatory, Sodankylä, Finland.

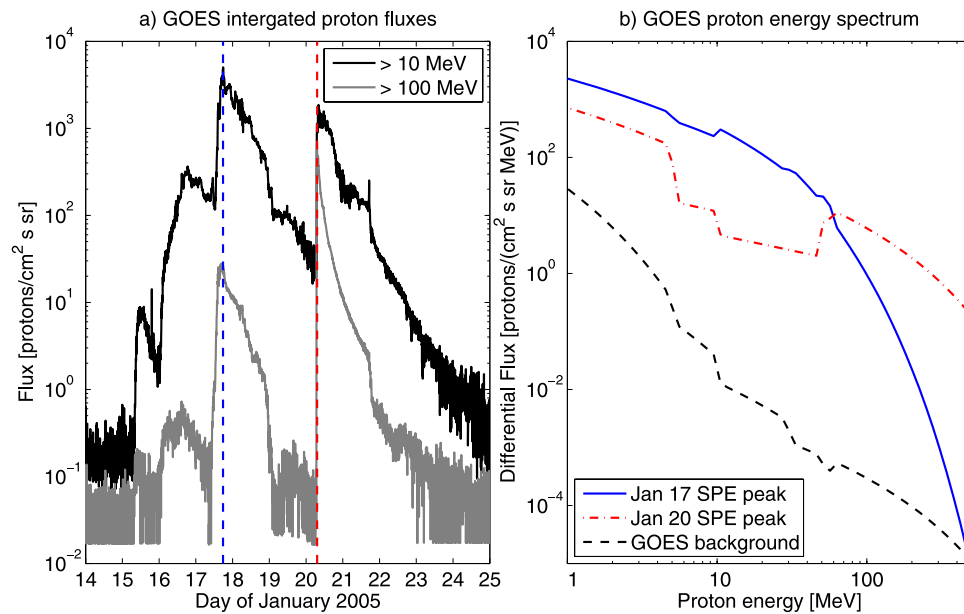


Figure 1. (a) GOES integrated proton fluxes at two different threshold energies ($>10 \text{ MeV}$ and $>100 \text{ MeV}$) for 14–24 January 2005. The dashed lines indicate the hard spectrum solar proton event of 20 January (red) and the preceding regular spectrum solar proton event of 17 January (blue). (b) Differential proton spectra of the hard spectrum event (red dash-dot line) and the regular spectrum event (blue solid line). The average GOES quiet time proton spectrum is presented for contrast (black dashed line).

unusual in that they included a period of very hard energy proton spectra on 20 January. While the fluxes of the lower energy protons were small, there were unusually high fluxes of high-energy protons, and thus this event was more likely to lead to effects at lower altitudes. Our aim is to contrast the effects of the hard-energy protons with those more typical for SPE, on both the winter (northern) and summer (southern) hemispheres. For this we will use the Sodankylä Ion and Neutral Chemistry model together with radio wave observations and modeling. Interhemispheric differences of the SPE impact have been investigated before [e.g., *Rohen et al.*, 2005; *Jackman et al.*, 2008], but to our knowledge not for short timescales and with a detailed ion and neutral chemistry model such as the one we have used in our study. For example, *Rohen et al.* [2005] have shown extensive interhemispheric comparisons of model results as well as observations, but focus on daily and zonally average results for their comparison with the satellite data. While *Jackman et al.* [2008] include some interhemispheric comparison of model results, their results are based on a climate model where the production of the key species HO_x and NO_x is parameterized. Similar parameterization is also used by *Rohen et al.* [2005]. Our ion and neutral chemistry model, on the other hand, calculates HO_x and NO_x production through ion chemistry.

2. January 2005 Solar Storms

[6] Early on 16 January 2005 a series of solar proton events began, following the X-class flare (X2.6: peak of $0.1\text{--}0.8 \text{ nm x-ray flux} = 2.6 \times 10^{-4} \text{ Wm}^{-2}$) observed on 15 January. A day later, on 17 January a yet stronger flare (X3.8) and associated CME were observed, followed by an even stronger flare (X7) and CME on 20 January. The

20 January X7 flare originated from the giant sunspot 720. From this flare began an extraordinary solar proton storm. The fluxes of solar protons with the highest energies (the $>100 \text{ MeV}$ proton fluxes as measured by the particle counters onboard the GOES-satellites) were of the same order as those observed during the well known October 1989 solar proton events [*Reid et al.*, 1991; *Zadorozhny et al.*, 1992; *Jackman et al.*, 1995], while the lower energy fluxes remained at moderate levels, making the 20 January event the hardest solar proton event observed in solar cycle 23. *Jackman et al.* [2008] have estimated the overall NO_y ($\text{NO}_x + \text{NO}_3 + 2 \text{ N}_2\text{O}_5 + \text{HNO}_3 + \text{HO}_2\text{NO}_2 + \text{ClONO}_2 + \text{BrONO}_2$) production from the solar proton events in January 2005 to be about 1.8 Gigamoles. On the basis of the level of NO_y production they ranked the January 2005 solar proton events as the 11th largest that has occurred in the past 45 years.

[7] The fluxes of protons at two different threshold energies are presented in Figure 1a. The two fluxes presented are the $>10 \text{ MeV}$ flux, which corresponds to protons that ionize the atmosphere mainly at altitudes of 65 km and above, and the $>100 \text{ MeV}$ flux, causing ionization mainly in the stratosphere, at altitudes of 30 km and above. Figure 1b presents the differential proton energy spectrum at two different peaks of the solar proton fluxes. The first spectrum is taken from the moderate solar proton event on 17 January and the second spectrum from the event of 20 January (timings indicated by dashed lines in Figure 1a). Both spectra correspond to the peak flux times of the respective solar proton events. The dashed line in Figure 1b corresponds to the quiet time GOES proton spectrum, representing the average GOES proton flux during non-disturbed times.

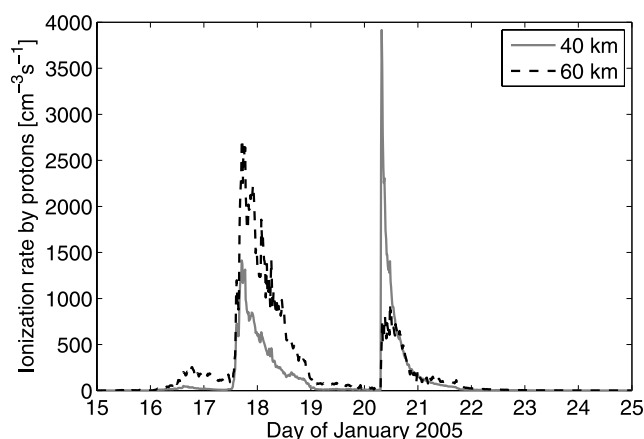


Figure 2. Calculated proton ionization rates at stratospheric (40 km, solid line) and mesospheric (60 km, dashed line) altitudes for 15–24 January.

[8] The hardness of the proton spectrum on 20 January caused the maximum ionization due to the proton precipitation to peak at stratospheric altitudes. Figure 2 presents the ionization rates, calculated using the GOES proton measurements, at representative stratospheric and mesospheric altitudes (40 and 60 km).

3. Sodankylä Ion and Neutral Chemistry Model

[9] The Sodankylä Ion and Neutral Chemistry model has been developed from the pure ion chemistry model presented by Turunen [1993] and is a one-dimensional model extending from the stratosphere up to 150 km altitude with 1 km vertical resolution. The model solves the concentrations of 64 ions (28 negative and 36 positive ions) and 15 neutral species. For a comprehensive list of model species see Verronen *et al.* [2006]. Several hundred chemical reactions are taken into account as well as external forcing due to solar radiation at 1–423 nm wavelengths, electron and proton precipitation, and galactic cosmic rays. Recent and extensive model descriptions are given by Verronen *et al.* [2005] and Verronen [2006].

[10] In this paper we use the model's time-dependent mode which exploits the semi-implicit Euler method for stiff sets of equations [Press *et al.*, 1992] to advance the concentrations of the constituents in time. The model includes a vertical transport scheme, as described by Chabrilat *et al.* [2002], which takes into account molecular and eddy diffusion. Within the transport code the molecular diffusion coefficients are calculated according to Banks and Kockarts [1973]. Eddy diffusion coefficient profile can be varied using the parameterization given by Shimazaki [1971]. Vertical transport and chemistry are advanced in 15 min intervals (with exponentially increasing time steps within each interval) during which the model background atmosphere and all external forcing are kept constant. In every interval the following steps are taken (1) all modeled neutrals, apart from the short-lived constituents $O(^1D)$ and $N(^2D)$, are transported, (2) new values for solar zenith angle, background atmosphere, and ionization/dissociation rates due to solar radiation and particle precipitation are calculated, and (3) the chemistry is advanced.

[11] For this study, we selected locations at the northern ($70^{\circ}N$, $0^{\circ}E$, $L \approx 7$) and southern hemisphere polar regions ($70^{\circ}S$, $45^{\circ}E$, $L \approx 7$) to examine the forcing of the hard spectrum events on the two hemispheres. The model vertical range was limited to altitudes below 120 km instead of the full model range to focus on the mesospheric-stratospheric altitudes. At the northern hemisphere modeling location there is low solar illumination throughout the modeling period, and even at 70 km there is <7 h of daylight on 24 January. Consequently, photodissociation, and photoionization processes take place only during these few sunlit hours. In the southern hemisphere the situation is the opposite with long sunlit days and only a few hours of darkness making the photochemical conditions of the two modeling locations very different.

[12] Before modeling the proton forcing effect of the solar proton events, the model was set up for quiet-time conditions equivalent to mid-January by repeating a diurnal cycle until convergence. Once convergence was reached, the model was run without the SPE proton forcing for the full length of the solar proton event modeling period as a control (i.e., quiet-time) run against which the SPE model runs will be contrasted later in this paper. For the SPE runs the model was provided with the proton flux measurements acquired from the geostationary GOES-11 satellite (available through the Space Physics Interactive Data Resource, <http://spidr.ngdc.noaa.gov>). Atmospheric ionization rates from the proton precipitation were then calculated following the approach presented by Verronen *et al.* [2005]. The proton fluxes were taken to be isotropic. The modeling locations correspond to high geomagnetic latitudes ($\sim 68^{\circ}N/S$) and therefore, to a first approximation, the geomagnetic rigidity cut-off effects of Rodger *et al.* [2006], Clilverd *et al.* [2007] can be neglected. The proton ionization rates for 40 and 60 km altitudes are shown in Figure 2.

[13] For both hemispheres the modeling begins at 0 UT on 15 January and continues until 26 January, 23:45 UT. The model runs with the proton forcing will be referred to as the proton runs, and those without proton forcing as the control runs.

4. Observations

[14] Very low frequency (VLF) radio wave propagation, occurring in the 3–30 kHz part of the electromagnetic spectrum, is used in communication systems, for example between ground stations and submarines. The signals are generated by high-power transmitters around the world. VLF signals generated by man-made transmitters propagate in the waveguide formed by the Earth's surface and the lower boundary of the ionosphere (D region) located between 50 and 100 km [Barr *et al.*, 2000], i.e., subionospherically. Therefore changes in the D-region ionosphere lead to changes in the amplitude and phase of the received VLF signals. As a consequence of the sensitivity to changes in the D-region electron density, VLF radio wave signals may be used to monitor changes in the sources of ionization, such as particle precipitation, in the mesosphere-lower thermosphere.

[15] The signals coming from distant transmitters can be monitored by VLF radio wave receivers set up in different locations around the Earth. In this study, we have used the

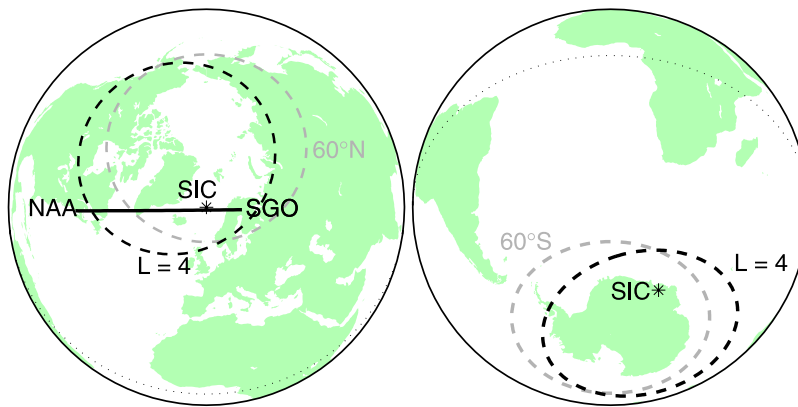


Figure 3. (left) Locations of the VLF transmitter (NAA) and receiver (Sodankylä, SGO) with the connecting great circle path and the ion and neutral chemistry modeling location (asterisk, SIC) in the northern polar area. (right) The ion and neutral chemistry modeling location (asterisk, SIC) in the southern polar area. The black dashed lines represent L-shells of 4.

VLF radio wave receiver located at Sodankylä, Finland (SGO, 67°N, 27°E, $L = 5.2$), to monitor the VLF signal coming from Cutler, Maine, USA (call sign NAA, 24 kHz). The great circle path from NAA to SGO, presented in Figure 3, crosses through the geomagnetic polar cap area (dashed line), close to the ion and neutral chemistry modeling location (asterisk), where the signal is influenced by ionospheric changes caused by the proton precipitation. The SGO site is part of the Antarctic-Arctic Radiation-belt Dynamic Deposition VLF Atmospheric Konsortia (AARDDVARK, M. A. Clilverd et al., Remote sensing space weather events: The AARDDVARK network, submitted to *Space Weather*, 2008, see the description of the array at http://www.physics.otago.ac.nz/space/AARDDVARK_homepage.htm).

[16] To study the signal propagation conditions we use the Long Wave Propagation Code (LWPC) [Ferguson and Snyder, 1990], provided by the Naval Ocean Systems Center to model the NAA VLF signal, analogously to Clilverd et al. [2005]. To calculate the signal amplitude and phase at the reception point LWPC needs electron density profile parameters that define the ionospheric conditions. These parameters are calculated from electron density profiles provided by the chemistry model results made during the proton run. Thus we are able to compare the observed NAA to SGO amplitude variations during SPE conditions with the output of the LWPC propagation model. The LWPC calculations are carried out for the NAA to Sodankylä propagation path, using the ion and neutral chemistry model electron density profiles to define the changing ionospheric conditions during the January 2005 solar proton events.

5. Results

5.1. Radio Wave Signal Modeling and Observations

[17] As described above, the ion and neutral chemistry model electron densities from the northern hemisphere runs were used in modeling the radio wave signal crossing the northern polar cap from NAA to SGO. The chemistry model control run results were first used to predict the radio wave Quiet Day Curve (QDC). These results are compared to the

observed QDC shown in Figure 4. The observed and modeled QDCs show very similar features corresponding to the signal amplitude diurnal variation and the amplitude levels compare well suggesting that the unperturbed D region ionosphere behavior is well captured by the ion and neutral chemistry model. Figure 4 (top) also presents the observed radio wave signal amplitude on 20 January. There is a sharp decrease of about 10 dB in the signal amplitude at 0715 UT corresponding to the onset of the hard spectrum solar proton event (Figure 1, dashed line on 20 January). Note that as the lower ionosphere is already affected by the decaying proton precipitation from the previous SPE, and as such the signal amplitude on 20 January is not expected to match the QDC amplitude. Figure 4 (bottom) presents the observed NAA to SGO radio wave amplitude change from the QDC amplitude together with the modeled amplitude change from 15 to 25 January. As in Figure 1, the SPE onset times corresponding to the proton flux increases on 16, 17 and 20 January are also shown. The observed amplitude change during the 20 January hard spectrum event (about -11 dB) is equivalent to the amplitude change during the earlier “softer” spectrum, higher flux event on 17 January (about -16 dB). The modeled radio wave signal captures the amplitude changes during the solar proton events very well. Both the observed signal and the modeled signal show similar return toward the QDC after the last solar proton event on 20 January.

5.2. Ion and Neutral Chemistry Modeling

[18] Figures 5–8 show the overall response of the northern and southern hemisphere NO_x ($\text{NO} + \text{NO}_2$), HO_x ($\text{OH} + \text{HO}_2$) and O_x ($\text{O} + \text{O}_3$) to the SPEs. The hemispheric differences are very striking for all three. The model results predict the main impact to take place at mesospheric altitudes; only HO_x in the northern hemisphere experiences large increases down to low stratospheric altitudes around 30 km. This happens during the hard spectrum event as well as during the earlier SPE on 17 January. The NO_x % increases at high mesospheric altitudes are much larger in the southern than the northern hemisphere. This is due to low NO_x in the summer polar mesosphere, leading to higher

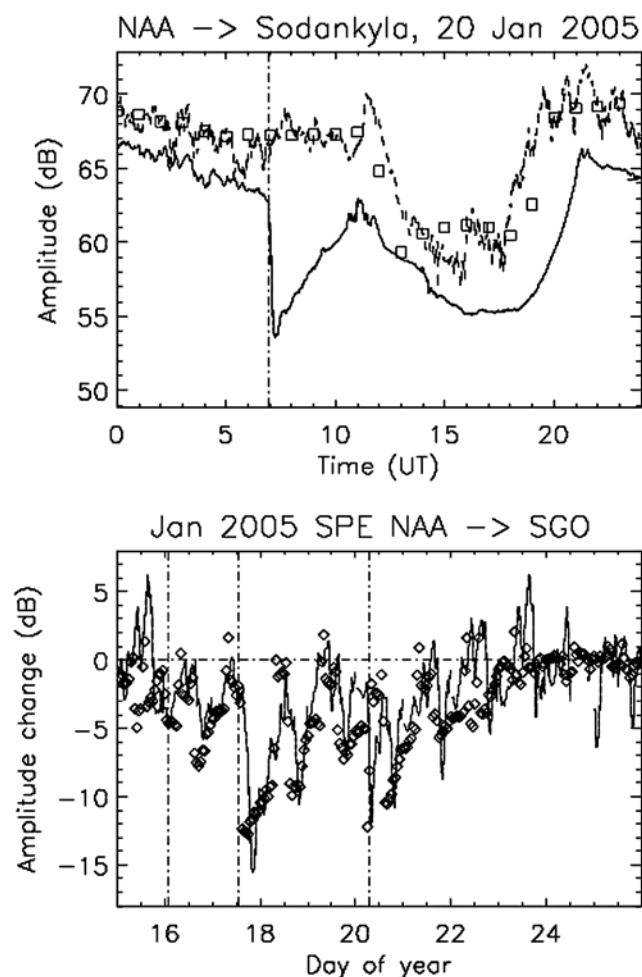


Figure 4. (top) Observed (dashed line) and modeled (squares) Quiet Day Curve (QDC) amplitude [dB] for the path from NAA to Sodankylä. The solid line is the observed amplitude during 20 January. The dash dot line marks the beginning of the hard spectrum event. (bottom) The observed (solid line) and the modeled (diamonds) amplitude change from the QDC for the NAA to Sodankylä (SGO) path from 15 to 25 January. The dash dot lines indicate the onset times of the three respective SPEs.

relative increases. Examination of the absolute increases (Figure 6) reveals that the initial NO_x productions on both hemispheres are quite similar with values of up to $1.4 \times 10^7 \text{ mol/cm}^3$ above 50 km predicted after the hard spectrum event. In the southern hemisphere the values start to decrease soon after the SPE forcing decays.

[19] Conversely, the southern hemisphere HO_x has a very minor response to the SPEs, even the HO_x increases from the hard spectrum event remain negligible. This is expected as the typical HO_x concentrations in the summer hemisphere are much larger than in the winter hemisphere—in contrast to the opposite situation for NO_x . Thus the southern hemisphere HO_x production from the SPEs remains relatively low. As the O_x amount in the mesosphere is largely controlled by reactions with HO_x , the predicted O_x losses are also smaller in the southern hemisphere, reflecting the relatively low SPE HO_x pro-

duction [Solomon *et al.*, 1983]. The region near 82 km altitude showing nearly continuous O_x loss corresponds to the mesospheric ozone minimum.

[20] For a further detailed examination of the impact of the SPEs on stratospheric and mesospheric altitudes two representative altitudes (40 and 60 km) were chosen. Figure 9 presents the northern hemisphere results for NO_x and ozone at 40 and 60 km altitudes from the ion and neutral chemistry model. The left and right sides of Figure 9 represent the percent-changes between the proton and control runs for NO_x and O_3 , respectively. In Figure 10 the southern hemisphere results are presented in the same format as the northern hemisphere results. Some aspects of the northern hemisphere results have previously been discussed by Seppälä *et al.* [2006].

[21] In both hemispheres there is significant NO_x production observed at mesospheric altitudes with the model results showing $>200\%$ NO_x increases above about 55 km. By 19 January the increase in NO_x is about 400% with respect to the control run and the hard-spectra SPE on 20 January further increases the NO_x production leading to an almost 500% total increase. In the sunlit summer southern pole the NO_x concentrations start to decay rapidly after the peak increase on 21 January and drop to values below 400% within three days of the largest increase. In the winter hemisphere the NO_x enhancement stabilizes after 21 January at about 460%. The most significant ozone responses to the solar proton events occur at high mesospheric altitudes (around 75 km) with ozone decreases up to 80% (see Figure 8). At 60 km up to 30–40% ozone loss is predicted for 19 and 21 January.

[22] In the stratosphere the NO_x production in both hemispheres is much lower than in the mesosphere and even though the hard spectrum event on 20 January results in a production peak, the NO_x enhancement remains below 20% in both hemispheres. In the summer hemisphere, where the initial NO_x concentrations are lower than in the winter hemisphere, there is slightly more relative NO_x production in the stratosphere.

[23] While the ozone loss in the model at high mesospheric altitudes is generally driven by HO_x , during the SPEs at 60 km altitudes the main nighttime ozone loss mechanisms turn out to be reactions of ozone with NO_x , which become the main nighttime ozone loss process from 19 January onward, with only a small contribution from HO_x . However, the main overall ozone loss still takes place during the daytime, when reactions with HO_x become the dominant ozone loss source [Verronen *et al.*, 2005]. This results in the rapid ozone loss at sunrise times seen in Figure 9. In the southern hemisphere, with very different solar illumination conditions, the largest ozone response according to the model takes place at around 75 km on 17–18 January, with up to 40% ozone decreases but lasting for a few hours only. At lower mesospheric altitudes (60 km) the largest ozone depletion is predicted to occur at the same time but the scale of this depletion is only about 15%. The hard spectrum event on 20 January has only a small effect, with about –4% change on ozone.

[24] At 40 km altitude in the stratosphere the total impact of the proton forcing on the ozone levels is very small. As might be expected, the hard spectrum event on 20 January has a distinct, although small, effect at stratospheric alti-

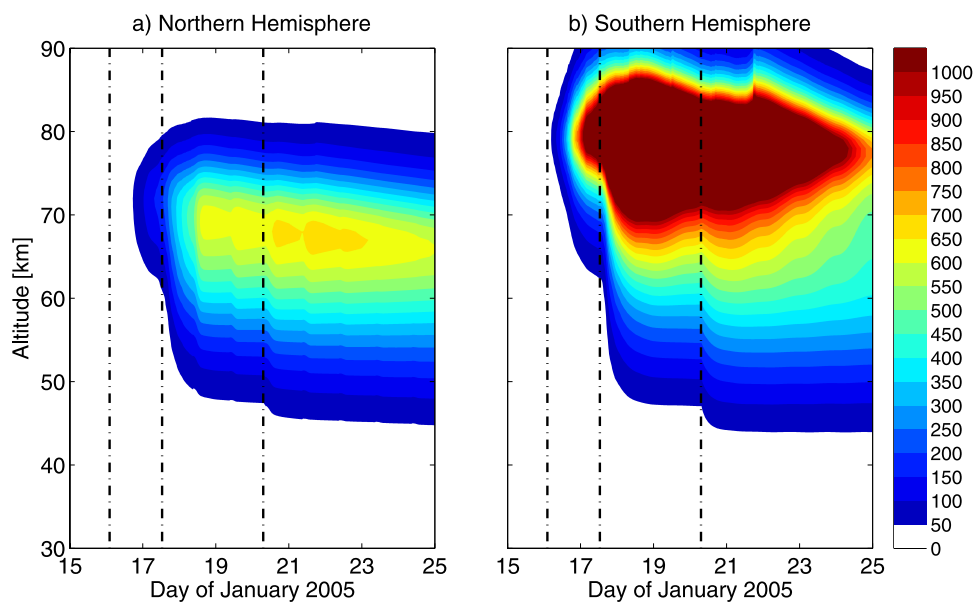


Figure 5. Increase of NO_x ($\text{NO} + \text{NO}_2$) in % due to the January 2005 SPEs (increase from control runs). (a) Northern hemisphere. (b) Southern hemisphere. The dash dot lines indicate the three SPE onset times.

tudes. With the maximum NO_x increases being only about 10–20% on both hemispheres throughout the SPE sequence, the predicted ozone changes are also small and of the order of <1%. In the summer hemisphere the ozone changes also reflect the changes in the solar zenith angle due to oxygen photochemistry processes.

6. Discussion

6.1. The Hard Spectrum Event

[25] Both hemispheres show similar stratospheric responses to the 20 January hard spectrum event with a sudden

increase in NO_x and a simultaneous decrease in ozone. As the photochemical lifetime of NO_x in the stratosphere is of the order of days to months [Brasseur and Solomon, 2005, pp. 341–343] this effect could potentially be long lasting and the modeled NO_x increases, although small, are still present up to the end of the modeling period.

[26] Even though the NO_x increases are long lasting in the stratosphere the ozone depleting effect of the hard spectrum event is very small (<1%). Although NO_x gases are important in determining the stratospheric ozone balance, the relative amount of NO_x produced by this event are too

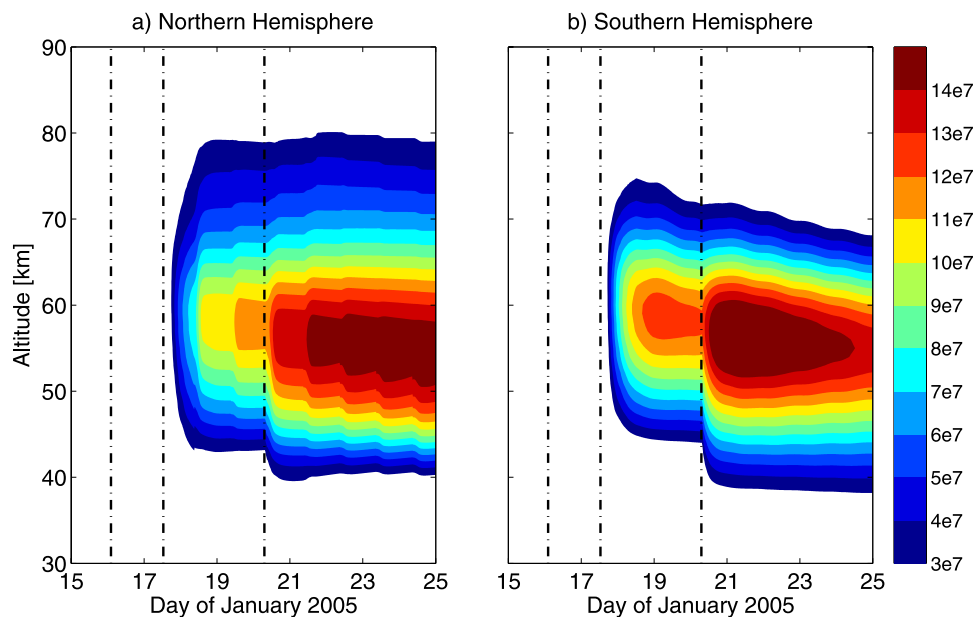


Figure 6. Increase of NO_x ($\text{NO} + \text{NO}_2$) in number density [mol/cm^3] due to the January 2005 SPEs (increase from control runs). (a) Northern hemisphere. (b) Southern hemisphere. The dash dot lines indicate the three SPE onset times. White areas are increases smaller than $3 \times 10^7 \text{ mol}/\text{cm}^3$.

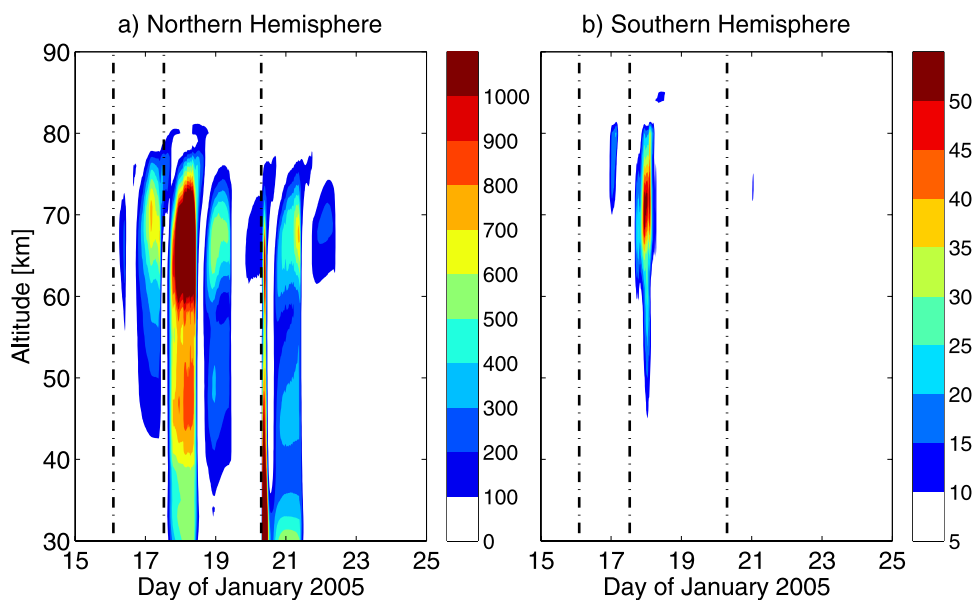


Figure 7. Increase of HO_x ($\text{HO} + \text{HO}_2$) in % due to SPE production (increase from control runs). (a) Northern hemisphere. (b) Southern hemisphere. The dash dot lines indicate the three SPE onset times.

low to contribute significantly to already occurring natural ozone loss in the upper stratosphere. How large would the high-energy proton fluxes need to be to produce enough NO_x and/or HO_x in the stratosphere to induce significant ozone loss at the same level as that predicted for the mesosphere? What if the hard spectrum proton forcing simply lasted for a longer time than it did for the 20 January event? Would there be enough stratospheric NO_x accumulation from a longer duration hard spectrum event? We examined these questions by introducing the observed proton spectrum from the hard spectrum event of 20 January shown in Figure 1b to the ion and neutral chemistry model

in the northern polar model point and maintaining the proton forcing for 24 hours. The results shown in Figure 11 indicated that although the amount of HO_x had increased by more than an order of magnitude below 50 km by the end of the 24 hour proton forcing period, and NO_x by about 50%, the impact on ozone still remained small (under 5%). This indicates that either considerably higher fluxes or a significantly longer event would be needed in order to produce enough NO_x to impact stratospheric ozone. An example of this type of situation would be the Carrington SPE that occurred in August/September 1859 [Carrington, 1859]. The possible impact that the Carrington event might have

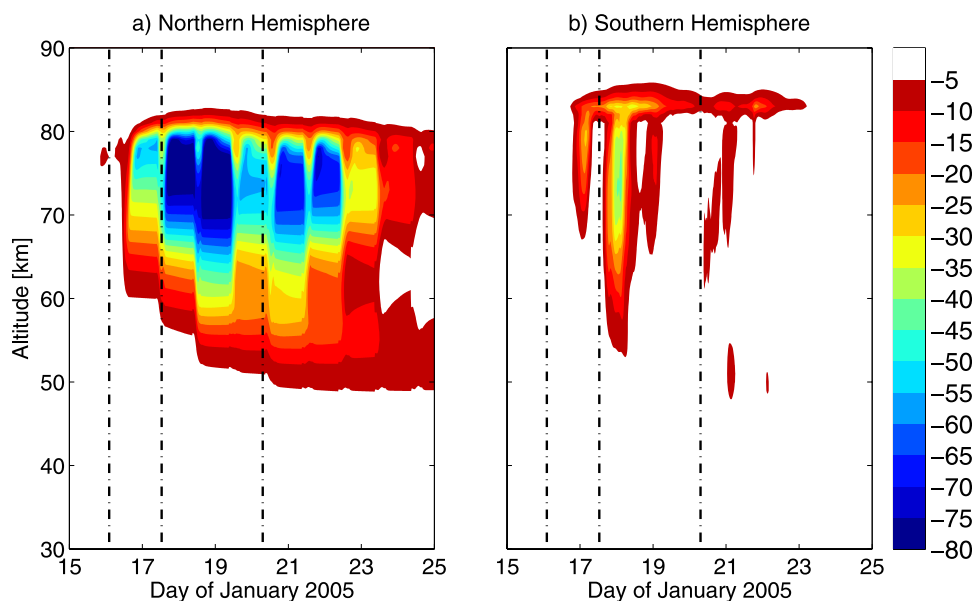


Figure 8. Change of O_3 ($\text{O} + \text{O}_3$) in % due to the SPEs (change from control runs). (a) Northern hemisphere. (b) Southern hemisphere. The dash dot lines indicate the three SPE onset times.

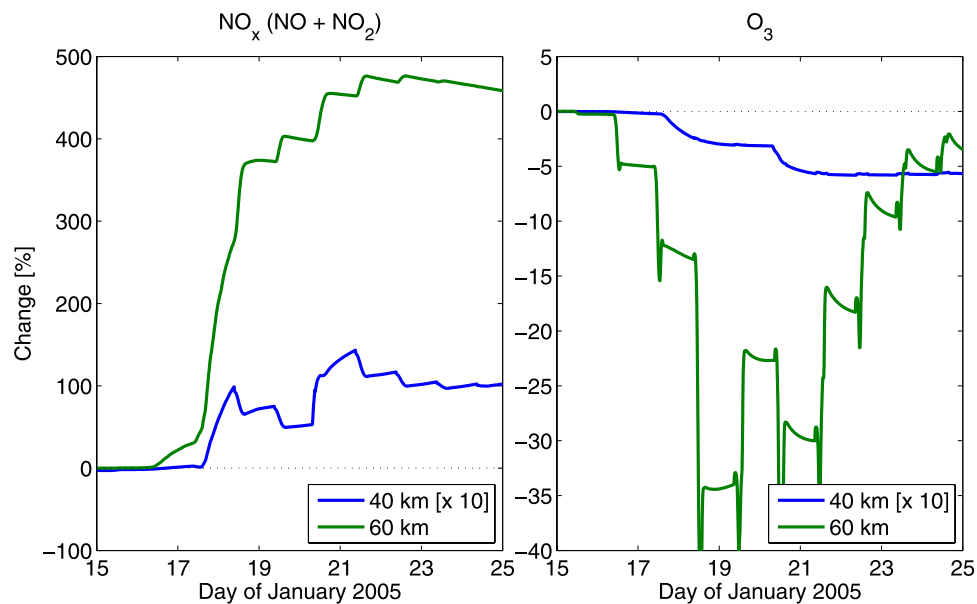


Figure 9. Northern hemisphere NO_x and O_3 response to the proton forcing during January at stratospheric (40 km) and mesospheric (60 km) altitudes. The values represent the % change from the model run without the proton forcing. Note that the stratospheric values at 40 km altitude have been multiplied by 10 to fit the 60 km NO_x and O_3 change scale.

had on the neutral atmosphere at the time has recently been studied with the Sodankylä Ion and Neutral Chemistry model by *Rodger et al.* [2008]. In this case a significant long-lasting decrease in stratospheric ozone is predicted, but for a SPE which is about 10 times bigger than the very large SPEs known from the “space age”. Modeling the long-term effects of these events would require a model that includes vertical as well as horizontal transport in the middle atmosphere (such as model used by *Thomas et al.*

[2007]). Thus such a case study is not viable with the 1-D SIC model.

6.2. The Overall SPE Response

[27] In the northern hemisphere winter at 70°N there is very little solar illumination throughout January as can be seen from Figure 12, showing the solar zenith angles calculated for the 40 km height. At 70°N the atmosphere is under nighttime conditions (zenith angles $>108^\circ$) for

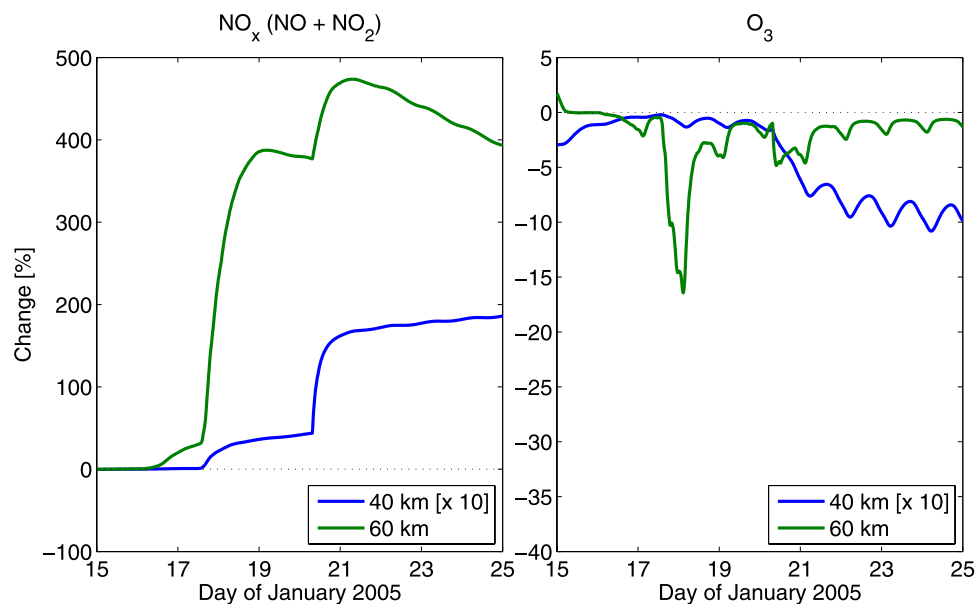


Figure 10. As Figure 9 but for southern hemisphere. Note that the stratospheric NO_x values at 40 km altitude have been multiplied by 10 to fit the 60 km NO_x change scale. The axis scales have been set to same values as in Figure 9 to aid the comparison between the two hemispheres.

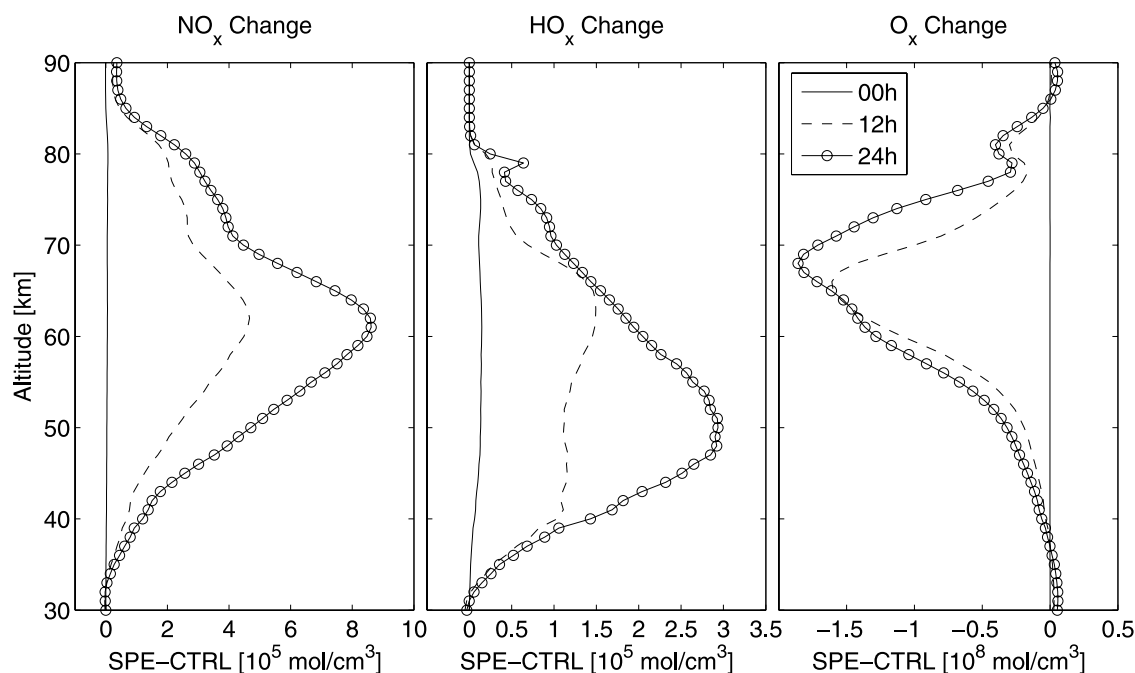


Figure 11. (From left to right) NO_x , HO_x , and O_3 change (from control runs) as a result of constant hard-spectra proton forcing at 70°N (see text). The profiles represent changes at midnight immediately after the forcing starts, at noon, and at midnight after 24 hours of hard proton forcing.

about 9 hours/day and under full solar illumination (zenith angles $<90^\circ$) with active photochemistry for only about 5 hours/day. At the same time the southern hemisphere at 70°S is under constant solar illumination with solar zenith angles of $<84^\circ$ at midnight. The different solar illumination conditions in the two polar regions are the primary reason for the different predicted SPE impacts as the level of SPE proton precipitation would not be expected to vary significantly from one geomagnetic pole to another.

[28] The model results indicate that the initial SPE-driven mesospheric NO_x production in the winter and summer polar regions are of similar levels, although in the summer mesosphere the ambient solar illumination rapidly leads to its decay. On longer timescales this has a significant effect on the different hemispheres as the SPE produced NO_x , which, having a long lifetime in the dark winter mesosphere, can affect the ozone balance first in the mesosphere and later in the stratosphere through downward transport processes. As the mesospheric O_3 balance is mainly determined by HO_x , larger ozone depletions in the mesosphere are predicted in the winter hemisphere where the relative HO_x production is significantly larger. This agrees well with recent polar observations and modeling of SPE impact [López-Puertas *et al.*, 2005; Rohen *et al.*, 2005]. For example, López-Puertas *et al.* reported ozone observations made right after the Halloween 2003 SPEs showing 50–70% depletion in the winter and 30–40% depletion in the summer lower mesosphere.

7. Conclusions

[29] In this paper we have examined the effects of the January 2005 solar proton events on the polar stratosphere and mesosphere with particular focus on the hard spectrum

event of 20 January. The effects were studied on both the winter northern hemisphere and the summer southern hemisphere atmospheres using ion and neutral chemistry modeling combined with radio wave propagation observation and modeling.

[30] The radio wave propagation observations showed significant impact from the 20 January hard spectrum event to the northern polar atmosphere, with radio wave amplitude changes of similar scale with the earlier moderate SPEs. The two weaker SPEs primarily ionized the mesosphere, rather than the stratosphere as the 20 January event did. Using ion

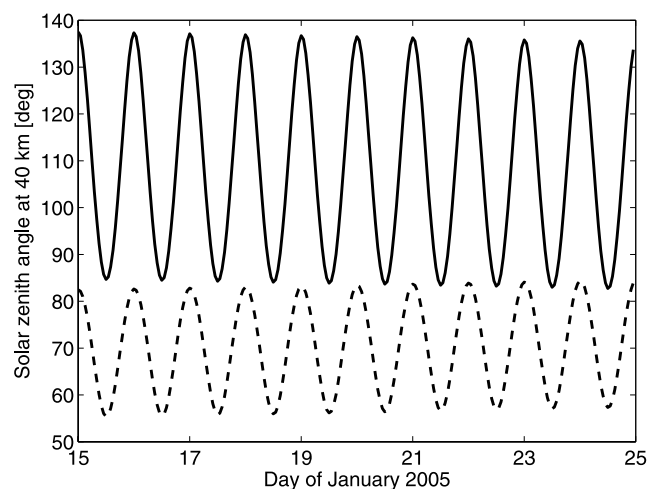


Figure 12. Solar zenith angles at model locations for 40 km altitude. Northern hemisphere: solid line. Southern hemisphere: dashed line.

and neutral chemistry modeling results as input to the LWPC radio wave propagation model we were able to reproduce the observed amplitude changes quite well. This indicated that with the inclusion of merely the proton precipitation (i.e., without any additional X-ray flare or electron precipitation input), the ion and neutral chemistry model is able to produce a reasonable ionospheric response to the January SPEs.

[31] The ion and neutral chemistry modeling which was carried out for a single representative location on both hemispheres (70°N/S) showed that the impact of the hard spectrum event on the polar stratosphere was small in both hemispheres. At mesospheric altitudes the impact of the three proton events was significant with about 500% increase in NO_x on both hemispheres. As a result, 30–40% ozone decreases lasting for a few days were predicted for the northern polar region and short-lived 15% ozone decreases for the southern polar region.

[32] At stratospheric altitudes the relative NO_x production from the SPEs was very small (10–20%) and therefore resulted in an insignificant effect on stratospheric ozone content. Our extreme case study indicated that a solar proton event with similar spectrum and flux to that of the 20 January but just with longer duration still did not create a significant instant impact on stratospheric ozone. Hard spectrum proton events with higher proton fluxes might induce significant instantaneous effects on stratospheric ozone.

[33] **Acknowledgments.** We are grateful to the Academy of Finland (EPPIC and THERMES), the New Zealand International Science and Technology Linkages Fund (ISAT), and the Lapland Atmosphere-Biosphere Facility (LAPBIAT2, Contract RITA-CT-2006-025969) for their generous support.

[34] Zuyin Pu thanks the reviewers for their assistance in evaluating this paper.

References

- Banks, P. M., and G. Kockarts (1973), *Aeronomy*, Elsevier, New York.
- Barr, R., D. L. Jones, and C. J. Rodger (2000), ELF and VLF radio waves, *J. Atmos. Terr. Phys.*, **62**, 1689–1718.
- Brasseur, G. P., and S. Solomon (2005), *Aeronomy of the Middle Atmosphere*, 3rd revised and enlarged ed., Springer, Dordrecht.
- Carrington, R. C. (1859), Description of a singular appearance seen in the Sun on September 1, 1859, *Mon. Not. R. Astron. Soc.*, **20**, 13–15.
- Chabrilat, S., G. Kockarts, D. Fonteyn, and G. Brasseur (2002), Impact of molecular diffusion on the CO₂ distribution and the temperature in the mesosphere, *Geophys. Res. Lett.*, **29**(15), 1729, doi:10.1029/2002GL015309.
- Clilverd, M. A., C. J. Rodger, T. Ulich, A. Seppälä, E. Turunen, A. Botman, and N. R. Thomson (2005), Modelling a large solar proton event in the southern polar atmosphere, *J. Geophys. Res.*, **110**, A09307, doi:10.1029/2004JA010922.
- Clilverd, M. A., C. J. Rodger, T. Moffat-Griffin, and P. T. Verronen (2007), Improved dynamic geomagnetic rigidity cutoff modelling: Testing predictive accuracy, *J. Geophys. Res.*, **112**, A08302, doi:10.1029/2007JA012410.
- Crutzen, P. J., I. S. A. Isaksen, and G. C. Reid (1975), Solar proton events: Stratospheric sources of nitric oxide, *Science*, **189**, 457–458.
- Ferguson, J. A., and F. P. Snyder (1990), Computer programs for assessment of long wavelength radio communications, *Tech. Doc. 1773*, Natl. Ocean Syst. Cent., Alexandria, Va.
- Jackman, C. H., M. C. Cerniglia, J. E. Nielsen, D. J. Allen, J. M. Zawodny, R. D. McPeters, A. R. Douglass, J. E. Rosenfield, and R. B. Hood (1995), Two-dimensional and three-dimensional model simulations, measurements, and interpretation of the October 1989 solar proton events on the middle atmosphere, *J. Geophys. Res.*, **100**, 11,641–11,660.
- Jackman, C. H., E. L. Fleming, and F. M. Vitt (2000), Influence of extremely large solar proton events in a changing stratosphere, *J. Geophys. Res.*, **105**, 11,659–11,670.
- Jackman, C. H., R. D. McPeters, G. J. Labow, E. L. Fleming, C. J. Praderas, and J. M. Russel (2001), Northern hemisphere atmospheric effects due to the July 2000 solar proton events, *Geophys. Res. Lett.*, **28**, 2883–2886.
- Jackman, C. H., et al. (2008), Short- and medium-term atmospheric constituent effects of very large solar proton events, *Atmos. Chem. Phys.*, **8**, 765–785.
- Lary, D. J. (1997), Catalytic destruction of stratospheric ozone, *J. Geophys. Res.*, **102**, 21,515–21,526.
- López-Puertas, M., B. Funke, S. Gil-López, T. v. Clarmann, G. P. Stiller, M. Höpfner, S. Kellmann, H. Fischer, and C. H. Jackman (2005), Observation of NO_x enhancement and ozone depletion in the northern and southern hemispheres after the October–November 2003 solar proton events, *J. Geophys. Res.*, **110**, A09S43, doi:10.1029/2005JA011050.
- McPeters, R. D., and C. H. Jackman (1985), The response of ozone to solar proton events during solar cycle 21: The observations, *J. Geophys. Res.*, **90**, 7945–7954.
- Patterson, J. D., T. P. Armstrong, C. M. Laird, D. L. Detrick, and A. T. Weatherwax (2001), Correlation of solar energetic protons and polar cap absorption, *J. Geophys. Res.*, **106**, 149–163.
- Press, W. H., S. A. Teukolsky, W. T. Vetterling, and B. P. Flannery (1992), *Numerical Recipes in FORTRAN, The Art of Scientific Computing*, Clarendon Press, Oxford, U.K.
- Randall, C. E., et al. (2005), Stratospheric effects of energetic particle precipitation in 2003–2004, *Geophys. Res. Lett.*, **32**, L05802, doi:10.1029/2004GL022003.
- Reames, D. V. (1999), Particle acceleration at the Sun and in the heliosphere, *Space Sci. Rev.*, **90**, 413–491.
- Reid, G. C., S. Solomon, and R. R. Garcia (1991), Response of the middle atmosphere to the solar proton events of August–December, 1989, *Geophys. Res. Lett.*, **18**, 1019–1022.
- Rodger, C. J., M. A. Clilverd, P. T. Verronen, T. Ulich, M. J. Jarvis, and E. Turunen (2006), Dynamic geomagnetic rigidity cutoff variations during a solar proton event, *J. Geophys. Res.*, **111**, A04222, doi:10.1029/2005JA011395.
- Rodger, C. J., P. T. Verronen, M. A. Clilverd, A. Seppälä, and E. Turunen (2008), The atmospheric impact of the Carrington event solar protons, *J. Geophys. Res.*, doi:10.1029/2008JD010702, in press.
- Rohen, G., et al. (2005), Ozone depletion during the solar proton events of October/November 2003 as seen by SCIAMACHY, *J. Geophys. Res.*, **110**, A09S39, doi:10.1029/2004JA010984.
- Rusch, D. W., J.-C. Gérard, S. Solomon, P. J. Crutzen, and G. C. Reid (1981), The effect of particle precipitation events on the neutral and ion chemistry of the middle atmosphere. I: Odd nitrogen, *Planet. Space Sci.*, **29**, 767–774.
- Seppälä, A., P. T. Verronen, E. Kyrölä, S. Hassinen, L. Backman, A. Hauchecorne, J. L. Bertaux, and D. Fussen (2004), Solar proton events of October–November 2003: Ozone depletion in the northern hemisphere polar winter as seen by GOMOS/Envisat, *Geophys. Res. Lett.*, **31**, L19107, doi:10.1029/2004GL021042.
- Seppälä, A., P. T. Verronen, V. F. Sofieva, J. Tamminen, E. Kyrölä, C. J. Rodger, and M. A. Clilverd (2006), Destruction of the tertiary ozone maximum during a solar proton event, *Geophys. Res. Lett.*, **33**, L07804, doi:10.1029/2005GL025571.
- Seppälä, A., M. A. Clilverd, and C. J. Rodger (2007), NO_x enhancements in the middle atmosphere during 2003–2004 polar winter: Relative significance of solar proton events and the aurora as a source, *J. Geophys. Res.*, **112**, D23303, doi:10.1029/2006JD008326.
- Shimazaki, T. (1971), Effective eddy diffusion coefficient and atmospheric composition in the lower thermosphere, *J. Atmos. Terr. Phys.*, **33**, 1383.
- Solomon, S., D. W. Rusch, J.-C. Gérard, G. C. Reid, and P. J. Crutzen (1981), The effect of particle precipitation events on the neutral and ion chemistry of the middle atmosphere. II: Odd hydrogen, *Planet. Space Sci.*, **8**, 885–893.
- Solomon, S., G. C. Reid, D. W. Rusch, and R. J. Thomas (1983), Mesospheric ozone depletion during the solar proton event of July 13, 1982: 2. Comparisons between theory and measurements, *Geophys. Res. Lett.*, **10**, 257–260.
- Thomas, B. C., C. H. Jackman, and A. L. Melott (2007), Modeling atmospheric effects of the September 1859 solar flare, *Geophys. Res. Lett.*, **34**, L06810, doi:10.1029/2006GL029174.
- Thomas, R. J., C. A. Barth, G. J. Rottman, D. W. Rusch, G. H. Mount, G. M. Lawrence, R. W. Sanders, G. E. Thomas, and L. E. Clemens (1983), Mesospheric ozone depletion during the solar proton event of July 13, 1982: 1. Measurement, *Geophys. Res. Lett.*, **10**, 253–255.
- Turunen, E. (1993), EISCAT incoherent scatter radar observations and model studies of day to twilight variations in the D region during the PCA event of August 1989, *J. Atmos. Terr. Phys.*, **55**, 767–781.
- Verronen, P. T. (2006), Ionosphere-atmosphere interaction during solar proton events, no. 55 in Finnish Meteorological Institute Contributions, Finnish Meteorological Institute, Helsinki, Doctoral thesis at the Univ. of Helsinki, Department of Physical Sciences. (Available at <http://ethesis.helsinki.fi>)

- Verronen, P. T., A. Seppälä, M. A. Clilverd, C. J. Rodger, E. Kyrölä, C.-F. Enell, T. Ulich, and E. Turunen (2005), Diurnal variation of ozone depletion during the October–November 2003 solar proton events, *J. Geophys. Res.*, *110*, A09S32, doi:10.1029/2004JA010932.
- Verronen, P. T., A. Seppälä, E. Kyrölä, J. Tamminen, H. M. Pickett, and E. Turunen (2006), Production of odd hydrogen in the mesosphere during the January 2005 solar proton event, *Geophys. Res. Lett.*, *33*, L24811, doi:10.1029/2006GL028115.
- Zadorozhny, A. M., G. A. Tuchkov, V. N. Kikthenko, J. Laštovička, J. Boška, and A. Novák (1992), Nitric oxide and lower ionosphere quantities during solar particle events of October 1989 after rocket and ground-based measurements, *J. Atmos. Terr. Phys.*, *54*, 183–192.
- M. A. Clilverd, Physical Sciences Division, Natural Environment Research Council, British Antarctic Survey, Madingley Road, Cambridge CB3 0ET, U.K. (macl@bas.ac.uk)
- C. J. Rodger, Department of Physics, University of Otago, P.O. Box 56, Dunedin, New Zealand. (crodder@physics.otago.ac.nz)
- A. Seppälä and P. T. Verronen, Finnish Meteorological Institute, P.O. Box 503, FI-00101 Helsinki, Finland. (annika.seppala@fmi.fi; pekka.verronen@fmi.fi)
- E. Turunen, Sodankylä Geophysical Observatory, Tähteläntie 62, FI-99600 Sodankylä, Finland. (esa@sgo.fi)